MECHANICS AND CONTROL
Vol. 32 No. 4 2013 http://dx.doi.org/10.7494/mech.2013.32.4.152

ROMAN PUTANOWICZ*, JAN JAŚKOWIEC*, PIOTR PLUCIŃSKI*, ANNA STANKIEWICZ*

FINITE ELEMENT IMPLEMENTATION OF NONLINEAR THERMO-ELASTICITY AS TYPICAL COUPLING OF DIFFUSION AND MOMENTUM BALANCE

ABSTRACT

The formulation and algorithmic aspects of nonlinear thermo-elasticity are reviewed in the paper. The attention is focused on coupling due to thermal expansion and temperature dependence of elastic model parameters, and on the consistent linearization of the ensuing nonlinear set of equations for two-field finite elements. Non-stationary heat flow, static loading and small strains are assumed. The solutions of some benchmark examples, obtained using the developed finite element environment FEMDK, are presented. The formulation has a more general application domain in the context of arbitrary coupling of a nonstationary diffusion proces and momentum balance.

Keywords: *thermo-elasticity, nonlinear problem, finite element methods, software*

NIELINIOWE PROBLEMY TERMOSPRĘŻYSTOŚCI

W artykule przedstawiono sformułowanie i aspekty algorytmizacji dla nieliniowych problemów termosprężystości. Skupiono się na problemie sprzężenia wynikającego z rozszerzalności cieplnej oraz zależności parametrów materiałowych od temperatury. Przeprowadzono konsystentną linearyzację nieliniowego układu równań opisującego rozpatrywany problem i zaproponowano dwupolowy element skończony. Rozważania dotyczą niestacjonarnego przepływu ciepła przy założeniu statycznego charakteru obciążeń mechanicznych oraz małych odkształceń. Przedstawiono rozwiązania wybranych zadań benchmarkowych. Obliczenia wykonano przy użyciu rozwijanego środowiska obliczeniowego FEMDK, opartego na metodzie elementów skończonych. Zaprezentowane sformułowanie może mieć bardziej ogólne zastosowanie dla dowolnego przypadku sprzężenia niestacjonarnego procesu dyfuzji z problemami opisywanymi przez równania bilansu pędu.

Słowa kluczowe: *termosprężystość, problem nieliniowy, metoda elementów skończonych, oprogramowanie*

1. INTRODUCTION

The aim of the paper is to present the formulation of nonlinear thermo-elasticity together with a suitable finite element algorithm for nonstationary processes and some examples of benchmark finite element computations. The computations are performed using software environment FEMDK which allows the analyst to consider various physical fields coupled to mechanics. The application domain are engineering materials, especially concrete, so eventually coupled processes such as the ones covered in monographs Gawin (2010); Kuhl (2005) are supposed to be analyzed.

The mechanical model considered in the paper is statics of nonlinearly elastic materials, but it is understood here as a prototype of a general nonlinear constitutive model for the solid skeleton of the material (with some additional complexity the model could incorporate damage, plasticity or cracking). On the other hand, the heat conduction model used in the paper, is a prototype of many nonstationary diffusion processes occurring in engineering materials, including moisture transport and related chemo-physical processes. This is because the partial differential equations governing the processes are quite similar.

A critical review of finite element analysis of solid thermomechanics is performed e.g. in Nicholson (2008). The thermodynamic foundations of the theory are covered for instance in Jirasek and Bažant (2002); Lemaitre and Chaboche (1990); Lubliner (1990); Maugin (1992); Ottosen and Ristinmaa (2005).

Static loading and linear kinematic equations are assumed in this paper. Small strain thermo-elasticity is a well-known theory. In this paper the aim is to incorporate arbitrary nonlinearity and coupling in the formulation. This means that nonlinear elasticity is admitted and, next to thermal expansion, the mechanical and thermal material properties (e.g. Young's modulus and/or conductivity) are considered as time and temperature-dependent.

The paper is organized as follows. In Section 2 the strong and weak forms of the mathematical model are reviewed for the simple coupling due to thermal expansion. Algorithmic aspects related to boundary conditions are mentioned. In Section 3 the formulation for nonlinear thermo-elasticity with temperature-dependent model parameters is covered. Algorithmic aspects related to time integration are discussed. The developed simulation environment FEMDK is briefly described in Section 4 and its features are listed. In Section 5 example solutions of coupled thermo-elasticity problems are presented. They concern stationary or non-stationary temperature and stress evolution in a bar, a square specimen and a thick-walled cylinder. Final remarks in Section 6 complete the paper.

2. REVIEW OF LINEAR THERMO-ELASTICITY

2.1. Mathematical model and discretization

Nonstationary heat transfer is described as follows, cf. Buckley (2010); Nicholson (2008).The balance equation, valid at each

* Institute for Computational Civil Engineering, Cracow University of Technology, ul. Warszawska 24, 31-155 Cracow, Poland; R.Putanowicz@L5.pk.edu.pl

point $\boldsymbol{x}$ in volume Ω at each time instant t from interval $[t_0, t_f]$, reads:

$$\rho c\dot{\Theta} + \nabla^{\mathrm{T}}\boldsymbol{q} = r \quad \forall \boldsymbol{x} \in \Omega \;\; \forall t \in [t_0, t_f] \tag{1}$$

where ρ [kg/m^3] is the density, c [J/(kg deg)] is the specific heat capacity, $\Theta = T - T_0$ [deg] is the relative temperature, i.e. its increase with respect to strain-free (initial, reference) temperature T_0, $\boldsymbol{q}$ [J/(m^2 s)] is the heat flux density, r [J/(m^3 s)] is the heat source density. Kelvin's effect is neglected, cf. Ottosen and Ristinmaa (2005). The balance equation incorporating the Fourier law $\boldsymbol{q} = -\boldsymbol{\Lambda}\nabla\Theta$ is written as:

$$\nabla^{\mathrm{T}}(\boldsymbol{\Lambda}\nabla\Theta) + r = \rho c\dot{\Theta} \tag{2}$$

where $\boldsymbol{\Lambda}$ [W/(m K)] is the thermal conductivity matrix.

For isotropic materials one can write this parabolic second order partial differential equation as:

$$\frac{\partial^2\Theta}{\partial x^2} + \frac{\partial^2\Theta}{\partial y^2} + \frac{\partial^2\Theta}{\partial z^2} + \frac{r}{k} = \rho c\frac{\partial\Theta}{\partial t} \tag{3}$$

where k [W/(m K)] is the thermal conductivity. The heat transport equation (2) or (3) must be complemented by proper initial and (essential or natural) boundary conditions. For stationary heat transfer the right-hand side is zero and the elliptic second order partial differential equation called Poisson equation is retrieved.

Before finite element discretization is used, the local model must be reworked into a global model in weak form:

$$\int_\Omega v_\Theta \rho c\dot{\Theta}\,\mathrm{d}\Omega + \int_\Omega (\nabla v_\Theta)^{\mathrm{T}}\boldsymbol{\Lambda}\nabla\Theta\,\mathrm{d}\Omega = \int_\Omega v_\Theta r\,\mathrm{d}\Omega - \int_\Gamma v_\Theta q_n\,\mathrm{d}\Gamma \quad \forall v_\Theta \in V_{\Theta,h} \tag{4}$$

where v_Θ is the weight function belonging to the space $V_{\Theta,h}$ of piecewise polynomials that vanish on Γ_Θ and $q_n = \boldsymbol{q}^{\mathrm{T}}\boldsymbol{n}$ denotes the heat flux normal to the body surface, assumed to be positive outwards ($\boldsymbol{n}$ is the vector normal to surface Γ). This integral equation must be valid together with essential boundary conditions $\Theta = \hat{\Theta}$ on Γ_Θ, while the natural boundary condition $q_n = \hat{q}_n$ on Γ_q is incorporated in eq. (4).

The standard equation of equilibrium (momentum balance) valid at each point of the considered isotropic solid is written as:

$$\boldsymbol{L}^{\mathrm{T}}\boldsymbol{\sigma} + \rho\boldsymbol{b} = \boldsymbol{0} \quad \forall \boldsymbol{x} \in \Omega \tag{5}$$

where $\boldsymbol{L}$ is the suitable differential operator matrix, $\boldsymbol{\sigma}$ is the stress tensor in vector form, $\boldsymbol{b}$ is the body force vector, usually related to gravitation. We limit our interest to linear elastic constitutive equations incorporating thermal expansion as initial strain

$$\boldsymbol{\sigma} = \boldsymbol{E}(\boldsymbol{\varepsilon} - \boldsymbol{\varepsilon}^{\Theta}), \quad \boldsymbol{\varepsilon}^{\Theta} = \alpha\Theta\boldsymbol{\Pi}, \quad \boldsymbol{\Pi} = [1\;1\;1\;0\;0\;0]^{\mathrm{T}} \tag{6}$$

where $\boldsymbol{E}$ is the Hooke operator, $\boldsymbol{\varepsilon}$ is the strain, α is the thermal expansion coefficient. One obtains the equilibrium equations as follows:

$$\boldsymbol{L}^{\mathrm{T}}\boldsymbol{E}\boldsymbol{\varepsilon} - \boldsymbol{L}^{\mathrm{T}}\boldsymbol{E}\alpha\Theta\boldsymbol{\Pi} + \rho\boldsymbol{b} = \boldsymbol{0} \tag{7}$$

The weak form of the equilibrium equation is the virtual work principle:

$$\int_\Omega (\boldsymbol{L}\boldsymbol{v}_{\mathrm{u}})^{\mathrm{T}}\boldsymbol{E}\boldsymbol{\varepsilon}\,\mathrm{d}\Omega - \int_\Omega (\boldsymbol{L}\boldsymbol{v}_{\mathrm{u}})^{\mathrm{T}}\boldsymbol{E}\alpha\Theta\boldsymbol{\Pi}\,\mathrm{d}\Omega = \int_\Omega \boldsymbol{v}_{\mathrm{u}}^{\mathrm{T}}\rho\boldsymbol{b}\,\mathrm{d}\Omega + \int_\Gamma \boldsymbol{v}_{\mathrm{u}}^{\mathrm{T}}\boldsymbol{t}\,\mathrm{d}\Gamma \quad \forall \boldsymbol{v}_{\mathrm{u}} \in V_{u,h} \tag{8}$$

where $\boldsymbol{t}$ is the traction vector and $\boldsymbol{v}_{\mathrm{u}}$ is the weight function belonging to the space $V_{u,h}$ of piecewise polynomials vanishing on Γ_u. This equation is valid together with essential boundary conditions $\boldsymbol{u} = \hat{\boldsymbol{u}}$ on Γ_u.

The following special cases of natural boundary conditions can be considered for the thermal sub-problem, cf. figure 1:

- convection $q_n = -h_c(T_c - T)$, where T_c is the absolute temperature of fluid moving around the sample, h_c [J/(m^{2}s)] is heat transfer coefficient;
- radiation or absorption $q_n = -h_r(T_r^4 - T^4)$, where T_r – absolute temperature of another body which radiates heat towards the considered body, h_r – emissivity coefficient (including Boltzmann constant). This case can be reformulated into the convection form of boundary conditions, but with a temperature-dependent heat transfer coefficient: $h_c = h_r(T_r^2 + T^2)(T_r + T)$.

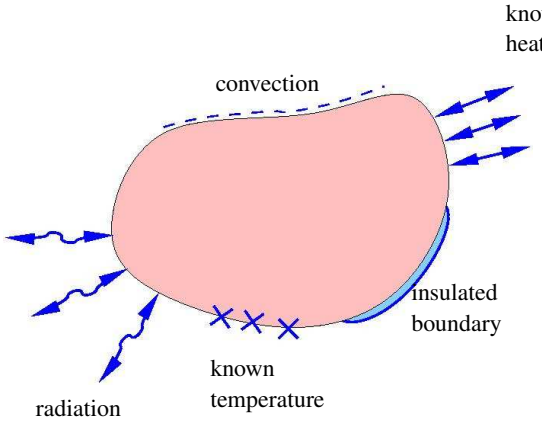

Fig. 1. Possible boundary conditions for heat transport problem

2.2. Algorithm and discretization – staggered scheme

The considered theory implies the solution of the evolutionary problem in time and space. The space discretization is provided by the FEM. We first focus on eq. (4) and introduce interpolation of the relative temperature as $\Theta = \boldsymbol{N}_\Theta\check{\boldsymbol{\Theta}}$, where $\boldsymbol{N}_\Theta$ denotes the shape function matrix and $\check{\boldsymbol{\Theta}}$ the vector of nodal temperature values.

This results in the following matrix equation:

$$\boldsymbol{C}\dot{\check{\boldsymbol{\Theta}}} + \boldsymbol{H}\check{\boldsymbol{\Theta}} = \boldsymbol{h}(t) \tag{9}$$

in which

$$\boldsymbol{C} = \int_{\Omega} \boldsymbol{N}_{\Theta}{}^{\mathrm{T}} \boldsymbol{N}_{\Theta} \rho c \, \mathrm{d}\Omega, \qquad \boldsymbol{H} = \int_{\Omega} \boldsymbol{B}_{\Theta}{}^{\mathrm{T}} \boldsymbol{\Lambda} \boldsymbol{B}_{\Theta} \, \mathrm{d}\Omega \tag{10}$$

are the heat capacity and conductivity matrices, respectively ($\boldsymbol{B}_{\Theta} = \nabla \boldsymbol{N}_{\Theta}$), and the right-hand side vector $\boldsymbol{h}$ reads:

$$\boldsymbol{h} = \int_{\Omega} \boldsymbol{N}_{\Theta}{}^{\mathrm{T}} r \, \mathrm{d}\Omega - \int_{\Gamma_q} \boldsymbol{N}_{\Theta}{}^{\mathrm{T}} \hat{q}_n \, \mathrm{d}\Gamma \tag{11}$$

Eq. (9) must be integrated over time. At time moment $t+\Delta t$ we have:

$$\boldsymbol{C} \dot{\check{\boldsymbol{\Theta}}}^{t+\Delta t} + \boldsymbol{H} \check{\boldsymbol{\Theta}}^{t+\Delta t} = \boldsymbol{h}^{t+\Delta t} \tag{12}$$

The temperature $\Theta^{t+\Delta t}$ can be represented by the generalized midpoint rule

$$\Theta^{t+\Delta t} = \Theta^{t} + \Delta t[(1-\gamma)\dot{\Theta}^{t} + \gamma \dot{\Theta}^{t+\Delta t}] \tag{13}$$

Different values of γ generate different algorithms (unconditionally stable backward Euler algorithm for $\gamma = 1$ is the most frequently used option).

For stationary heat transfer eq. (9) simplifies to:

$$\boldsymbol{H} \check{\boldsymbol{\Theta}} = \boldsymbol{h} \tag{14}$$

If the convection boundary condition is used with the heat transfer equation, then new arrays emerge with integrals over the relevant part of the body surface:

$$(\boldsymbol{H} + \boldsymbol{H}_c) \check{\boldsymbol{\Theta}} = \boldsymbol{h} + \boldsymbol{h}_c \tag{15}$$

where

$$\boldsymbol{H}_c = \int_{\Gamma_c} \boldsymbol{N}_{\Theta}{}^{\mathrm{T}} \boldsymbol{N}_{\Theta} h_c \, \mathrm{d}\Gamma, \quad \boldsymbol{h}_c = \int_{\Gamma_c} \boldsymbol{N}_{\Theta}{}^{\mathrm{T}} h_c (T_c - T_0) \, \mathrm{d}\Gamma \tag{16}$$

If the radiation boundary conditions are used for the heat transfer equation, then the problem becomes nonlinear and an incremental-iterative solution is necessary.

For the coupled model the discretization (global approximation) of the displacements $\boldsymbol{u} = \boldsymbol{N}_u \check{\boldsymbol{u}}$ and the temperature $\Theta = \boldsymbol{N}_{\Theta} \check{\boldsymbol{\Theta}}$, as well as the respective weighting functions in the Galerkin manner, lead to:

$$\begin{bmatrix} \boldsymbol{0} & \boldsymbol{0} \\ \boldsymbol{0} & \boldsymbol{C} \end{bmatrix} \begin{bmatrix} \dot{\check{\boldsymbol{u}}} \\ \dot{\check{\boldsymbol{\Theta}}} \end{bmatrix} + \begin{bmatrix} \boldsymbol{K} & \boldsymbol{K}_{\Theta} \\ \boldsymbol{0} & \boldsymbol{H} \end{bmatrix} \begin{bmatrix} \check{\boldsymbol{u}} \\ \check{\boldsymbol{\Theta}} \end{bmatrix} = \begin{bmatrix} \boldsymbol{f} \\ \boldsymbol{h} \end{bmatrix} \tag{17}$$

where

$$\begin{aligned} \boldsymbol{K}_{\Theta} &= \int_{\Omega} \boldsymbol{B}_u{}^{\mathrm{T}} \boldsymbol{E} \alpha \boldsymbol{\Pi} \boldsymbol{N}_{\Theta} \, \mathrm{d}\Omega, \\ \boldsymbol{f} &= \int_{\Omega} \boldsymbol{N}_u{}^{\mathrm{T}} \rho \boldsymbol{b} \, \mathrm{d}\Omega + \int_{\Gamma} \boldsymbol{N}_u{}^{\mathrm{T}} \boldsymbol{t} \, \mathrm{d}\Gamma \end{aligned} \tag{18}$$

and $\boldsymbol{B}_u = \boldsymbol{L}\boldsymbol{N}_u$. It is noted that the coupling is in one direction and the two matrix equations can be decoupled. This means a staggered scheme of solution can be adopted, i.e. first the thermal sub-problem is solved to obtain the temperature distributions at the assumed set of time instances and then the mechanical sub-problem is solved to obtain the evolution of the temperature-dependent stresses in time.

3. NONLINEAR THERMO-ELASTICITY

3.1. Mathematical model and discretization

The mechanical and thermal material properties (e.g. Young's modulus and/or conductivity) are now considered as time and temperature-dependent, possibly in a nonlinear manner.

We start the derivation from the mechanical part. It is assumed that $\rho\boldsymbol{b}, \boldsymbol{t}$ are independent of temperature, and also $\alpha = \text{const}$.

The equilibrium equation (5) holds:

$$\boldsymbol{L}^{\mathrm{T}} \boldsymbol{\sigma} + \rho \boldsymbol{b} = \boldsymbol{0} \qquad \text{in } \Omega \tag{19}$$

and so do the natural boundary conditions

$$\mathscr{N} \boldsymbol{\sigma} = \boldsymbol{t} \qquad \text{on } \Gamma_{\sigma} \tag{20}$$

where matrix $\mathscr{N}$ contains components of normal vector $\boldsymbol{n}$ properly arranged.

We can now consider linear elasticity with temperature-dependent Hooke operator:

$$\boldsymbol{\sigma} = \boldsymbol{E}(\boldsymbol{\varepsilon} - \boldsymbol{\varepsilon}^{\Theta}), \quad \boldsymbol{\varepsilon}^{\Theta} = \alpha \Theta \boldsymbol{\Pi}, \quad \boldsymbol{E} = \boldsymbol{E}(\Theta) \tag{21}$$

or admit a general form of nonlinear elasticity

$$\boldsymbol{\sigma} = \boldsymbol{\sigma}(\boldsymbol{\varepsilon}^{e}, \Theta), \quad \boldsymbol{\varepsilon}^{e} = \boldsymbol{\varepsilon} - \boldsymbol{\varepsilon}^{\Theta}, \quad \Theta = T - T_0 \tag{22}$$

We will further call $\boldsymbol{\varepsilon} = \boldsymbol{\varepsilon}^{e} + \boldsymbol{\varepsilon}^{\Theta}$ total strain and $\boldsymbol{\varepsilon}^{e}$ elastic strain.

Next, we write the weak form of equilibrium equations at time $t+\Delta t$ (note that essential boundary conditions hold $\boldsymbol{u} = \hat{\boldsymbol{u}}, \boldsymbol{v}_{\mathrm{u}} = 0$ on Γ_u):

$$\int_{\Omega} (\boldsymbol{L}\boldsymbol{v}_{\mathrm{u}})^{\mathrm{T}} \boldsymbol{\sigma} \, \mathrm{d}\Omega = \int_{\Omega} \boldsymbol{v}_{\mathrm{u}}^{\mathrm{T}} \rho \boldsymbol{b} \, \mathrm{d}\Omega + \int_{\Gamma_{\sigma}} \boldsymbol{v}_{\mathrm{u}}^{\mathrm{T}} \boldsymbol{t} \, \mathrm{d}\Gamma, \qquad \forall \boldsymbol{v}_{\mathrm{u}} \in V_{u,h} \tag{23}$$

The stress is additively decomposed:

$$\boldsymbol{\sigma}^{t+\Delta t} = \boldsymbol{\sigma}^{t} + \Delta \boldsymbol{\sigma} \tag{24}$$

and substituted into eq. (23) to obtain

$$\int_{\Omega} (\boldsymbol{L}\boldsymbol{v}_{\mathrm{u}})^{\mathrm{T}} \Delta \boldsymbol{\sigma} \, \mathrm{d}\Omega = W_{\mathrm{ext}}^{t+\Delta t} - W_{\mathrm{int}}^{t} \tag{25}$$

where $W_{\mathrm{ext}}^{t+\Delta t}$ is defined by the right-hand side of eq. (23) and W_{int}^{t} is as follows:

$$W_{\mathrm{int}}^{t} = \int_{\Omega} (\boldsymbol{L}\boldsymbol{v}_{\mathrm{u}})^{\mathrm{T}} \boldsymbol{\sigma}^{t} \, \mathrm{d}\Omega \tag{26}$$

The linearization is then performed at time $t+\Delta t$:

$$\Delta \boldsymbol{\sigma}_{i+1} = \Delta \boldsymbol{\sigma}_i + \delta \boldsymbol{\sigma}, \quad \boldsymbol{\sigma}_i^{t+\Delta t} = \boldsymbol{\sigma}^{t} + \Delta \boldsymbol{\sigma}_i \tag{27}$$

where $\delta\boldsymbol{\sigma}$ denotes the corrective increment of stress, and upon substitution into eq. (25) we obtain

$$\int_{\Omega} (\boldsymbol{L}\boldsymbol{v}_{\mathrm{u}})^{\mathrm{T}}\, \delta\boldsymbol{\sigma}\, \mathrm{d}\Omega = W_{\mathrm{ext}}^{t+\Delta t} - W_{\mathrm{int},i}^{t+\Delta t} \tag{28}$$

The corrective increment can be derived the same way as differential of a quantity is computed. The correction of stress is:

$$\delta\boldsymbol{\sigma} = \boldsymbol{E}\left(\delta\boldsymbol{\varepsilon} - \delta\boldsymbol{\varepsilon}^{\Theta}\right) + \delta\boldsymbol{E}\left(\boldsymbol{\varepsilon} - \boldsymbol{\varepsilon}^{\Theta}\right) \tag{29}$$

Further computation of $\delta\boldsymbol{E}$ and $\delta\boldsymbol{\varepsilon}^{\Theta}$

$$\delta\boldsymbol{E} = \frac{\mathrm{d}\boldsymbol{E}}{\mathrm{d}\Theta}\delta\Theta, \quad \delta\boldsymbol{\varepsilon}^{\Theta} = \alpha\,\delta\Theta\boldsymbol{\Pi} \tag{30}$$

leads to the formula for $\delta\boldsymbol{\sigma}$ for linear elasticity:

$$\delta\boldsymbol{\sigma} = \boldsymbol{E}\,\delta\boldsymbol{\varepsilon} + \boldsymbol{e}\,\delta\Theta \tag{31}$$

in which vector $\boldsymbol{e}$

$$\boldsymbol{e} = \frac{\mathrm{d}\boldsymbol{E}}{\mathrm{d}\Theta}(\boldsymbol{\varepsilon} - \alpha\Theta\boldsymbol{\Pi}) - \alpha\boldsymbol{E}\boldsymbol{\Pi} \tag{32}$$

is responsible for thermal expansion. The calculation can be repeated for nonlinear elasticity as shown in the next three lines:

$$\delta\boldsymbol{\sigma} = \frac{\partial\boldsymbol{\sigma}}{\partial\boldsymbol{\varepsilon}^{e}}\mathrm{d}\boldsymbol{\varepsilon}^{e} + \frac{\partial\boldsymbol{\sigma}}{\partial\Theta}\delta\Theta = \boldsymbol{E}_{\mathrm{T}}\,\delta\boldsymbol{\varepsilon}^{e} + \boldsymbol{\sigma}_{\Theta}\,\delta\Theta \tag{33}$$

$$\delta\boldsymbol{\varepsilon}^{e} = \delta\boldsymbol{\varepsilon} - \alpha\,\delta\Theta\boldsymbol{\Pi}, \qquad \boldsymbol{E}_{\mathrm{T}} = \left.\frac{\partial\boldsymbol{\sigma}}{\partial\boldsymbol{\varepsilon}^{e}}\right|_{\Theta=\mathrm{const}}, \qquad \boldsymbol{\sigma}_{\Theta} = \left.\frac{\partial\boldsymbol{\sigma}}{\partial\Theta}\right|_{\boldsymbol{\varepsilon}^{e}=\mathrm{const}} \tag{34}$$

$$\delta\boldsymbol{\sigma} = \boldsymbol{E}_{\mathrm{T}}\,\delta\boldsymbol{\varepsilon} + \boldsymbol{e}\,\delta\Theta, \qquad \boldsymbol{e} = \boldsymbol{\sigma}_{\Theta} - \alpha\boldsymbol{E}_{\mathrm{T}}\boldsymbol{\Pi} \tag{35}$$

Eq. (31) has a similar form to eq. (35), so the latter one will be used in further derivation.

The weak form of the equilibrium equation finally reads:

$$\int_{\Omega} (\boldsymbol{L}\boldsymbol{v}_{\mathrm{u}})^{\mathrm{T}}\boldsymbol{E}_{\mathrm{T}}\,\delta\boldsymbol{\varepsilon}\,\mathrm{d}\Omega + \int_{\Omega} (\boldsymbol{L}\boldsymbol{v}_{\mathrm{u}})^{\mathrm{T}}\boldsymbol{e}\,\delta\Theta\,\mathrm{d}\Omega = W_{\mathrm{ext}}^{t+\Delta t} - W_{\mathrm{int},i}^{t+\Delta t} \tag{36}$$

The non-stationary heat transport problem is reconsidered next. For simplicity it is assumed that ρ, c, r, $\hat{q}_n$ are independent of temperature. We recall that the energy balance gives:

$$\rho c\dot{\Theta} + \nabla^{\mathrm{T}}\boldsymbol{q} = r, \qquad \text{in } \Omega \tag{37}$$

and the natural boundary condition is

$$\boldsymbol{q}^{\mathrm{T}}\boldsymbol{n} = \hat{q}_n, \qquad \text{on } \Gamma_q \tag{38}$$

The Fourier law is assumed to be valid with temperature-dependent conductivity

$$\boldsymbol{q} = -\boldsymbol{\Lambda}\nabla\Theta, \qquad \boldsymbol{\Lambda} = \boldsymbol{\Lambda}(\Theta) \tag{39}$$

but another constitutive equation could also be used here.

The weak form of eq. (37) at time $t+\Delta t$ with the essential boundary conditions $\Theta = \hat{\Theta}, v_{\Theta} = 0$ on Γ_{Θ} satisfied reads:

$$\int_{\Omega} v_{\Theta}\rho c\dot{\Theta}\,\mathrm{d}\Omega - \int_{\Omega} (\nabla v_{\Theta})^{\mathrm{T}}\boldsymbol{q}\,\mathrm{d}\Omega = \int_{\Omega} v_{\Theta} r\,\mathrm{d}\Omega - \int_{\Gamma_q} v_{\Theta}\hat{q}_n\,\mathrm{d}\Gamma \qquad \forall v_{\Theta} \in V_{\Theta,h} \tag{40}$$

Adopting the generalized mid-point rule for time integration

$$\Theta^{t+\Delta t} = \Theta^{t} + (1-\gamma)\Delta t\dot{\Theta}^{t} + \gamma\Delta t\dot{\Theta}^{t+\Delta t} \tag{41}$$

the following incremental decompositions are obtained for $\gamma = 1$, i.e. for the backward Euler time integration:

$$\Theta^{t+\Delta t} = \Theta^{t} + \Delta t\dot{\Theta}^{t+\Delta t} \rightarrow \dot{\Theta}^{t+\Delta t} = \frac{\Delta\Theta}{\Delta t} \tag{42}$$

$$\boldsymbol{q}^{t+\Delta t} = \boldsymbol{q}^{t} + \Delta\boldsymbol{q}, \qquad \dot{\Theta}^{t+\Delta t} = \dot{\Theta}^{t} + \Delta\dot{\Theta} \tag{43}$$

Eq. (40) can now be rewritten as

$$\int_{\Omega} v_{\Theta}\rho c\frac{\Delta\Theta}{\Delta t}\,\mathrm{d}\Omega - \int_{\Omega} (\nabla v_{\Theta})^{\mathrm{T}}\Delta\boldsymbol{q}\,\mathrm{d}\Omega = Q_{\mathrm{ext}}^{t+\Delta t} - \int_{\Omega} (\nabla v_{\Theta})^{\mathrm{T}}\boldsymbol{q}^{t}\,\mathrm{d}\Omega \tag{44}$$

where $Q_{\mathrm{ext}}^{t+\Delta t}$ denotes the right hand of eq. (40).

The linearization of the equations at time $t+\Delta t$ means the following increment update:

$$\Delta\Theta_{i+1} = \Delta\Theta_i + \delta\Theta, \quad \Delta\boldsymbol{q}_{i+1} = \Delta\boldsymbol{q}_i + \delta\boldsymbol{q}, \qquad \boldsymbol{q}_i^{t+\Delta t} = \boldsymbol{q}^{t} + \Delta\boldsymbol{q}_i \tag{45}$$

in which the heat flux correction is calculated as

$$\delta\boldsymbol{q} = -\frac{\mathrm{d}\boldsymbol{\Lambda}}{\mathrm{d}\Theta}\nabla\Theta\,\delta\Theta - \boldsymbol{\Lambda}\nabla(\delta\Theta) \tag{46}$$

For simplicity we assume now that the conductivity does not depend on temperature:

$$\frac{\mathrm{d}\boldsymbol{\Lambda}}{\mathrm{d}\Theta} = 0, \quad \delta\boldsymbol{q} = -\boldsymbol{\Lambda}\nabla(\delta\Theta) \tag{47}$$

If this assumption is not true, an additional term occurs in the weak form. Upon substitution of eq. (47) into eq. (44), the following integral equation is obtained:

$$\frac{1}{\Delta t}\int_{\Omega} v_{\Theta}\rho c\mathrm{d}\Theta\,\mathrm{d}\Omega + \int_{\Omega} (\nabla v_{\Theta})^{\mathrm{T}}\boldsymbol{\Lambda}\nabla(\delta\Theta)\,\mathrm{d}\Omega = Q_{\mathrm{ext}}^{t+\Delta t} - Q_{\mathrm{int},i}^{t+\Delta t} \tag{48}$$

where

$$Q_{\mathrm{int},i}^{t+\Delta t} = -\int_{\Omega} (\nabla v_{\Theta})^{\mathrm{T}}\boldsymbol{q}_i\,\mathrm{d}\Omega + \frac{1}{\Delta t}\int_{\Omega} v_{\Theta}\rho c\Delta\Theta_i\,\mathrm{d}\Omega \tag{49}$$

A generalization of the mathematical formulation of multi-field problems can be found for instance in Kuhl (2005), while the extension of the theory to multicomponent materials (together with its thermodynamic background) is presented for instance in Kubik (2004).

3.2. Algorithm and discretization – monolithic scheme

Although for one-direction coupling this is not mandatory, a monolithic solution scheme is now proposed, in which two-field finite elements are used and the problem is solved simultaneously for both fundamental unknowns, i.e. the temperature and the displacement vector. The discretization of $\boldsymbol{u}$ and $\boldsymbol{v}_{\mathrm{u}}$ using $\boldsymbol{N}_u$ is performed, in particular $\boldsymbol{u} = \boldsymbol{N}_u \check{\boldsymbol{u}}$, $\boldsymbol{B}_u = \boldsymbol{L}\boldsymbol{N}_u$. Moreover, Θ and v_Θ are discretized using $\boldsymbol{N}_\Theta$, so that $\Theta = \boldsymbol{N}_\Theta \check{\boldsymbol{\Theta}}$, $\boldsymbol{B}_\Theta = \nabla \boldsymbol{N}_\Theta$. The substitution of the interpolation formula into the weak-form equations of equilibrium and energy balance leads to the following matrix equation:

$$\begin{bmatrix} \boldsymbol{K}_{\mathrm{T}} & \boldsymbol{K}_\Theta \\ \boldsymbol{0} & \boldsymbol{C}+\boldsymbol{H} \end{bmatrix} \begin{bmatrix} \delta\check{\boldsymbol{u}} \\ \delta\check{\boldsymbol{\Theta}} \end{bmatrix} = \begin{bmatrix} \boldsymbol{f}_{\mathrm{ext}}^{t+\Delta t} - \boldsymbol{f}_{\mathrm{int},i}^{t+\Delta t} \\ \boldsymbol{h}_{\mathrm{ext}}^{t+\Delta t} - \boldsymbol{h}_{\mathrm{int},i}^{t+\Delta t} \end{bmatrix} \tag{50}$$

where

$$\boldsymbol{K}_{\mathrm{T}} = \int_\Omega \boldsymbol{B}_u{}^{\mathrm{T}} \boldsymbol{E}_{\mathrm{T}} \boldsymbol{B}_u \,\mathrm{d}\Omega, \quad \boldsymbol{K}_\Theta = \int_\Omega \boldsymbol{B}_u{}^{\mathrm{T}} \boldsymbol{e} \boldsymbol{N}_\Theta \,\mathrm{d}\Omega$$

$$\boldsymbol{C} = \frac{1}{\Delta t} \int_\Omega \boldsymbol{N}_\Theta{}^{\mathrm{T}} \rho c \boldsymbol{N}_\Theta \,\mathrm{d}\Omega, \quad \boldsymbol{H} = \int_\Omega \boldsymbol{B}_\Theta{}^{\mathrm{T}} \boldsymbol{\Lambda} \boldsymbol{B}_\Theta \,\mathrm{d}\Omega$$

$$\boldsymbol{f}_{\mathrm{int},i}^{t+\Delta t} = \int_\Omega \boldsymbol{B}_u{}^{\mathrm{T}} \boldsymbol{\sigma}_i^{t+\Delta t} \,\mathrm{d}\Omega,$$

$$\boldsymbol{h}_{\mathrm{int},i}^{t+\Delta t} = \int_\Omega \boldsymbol{N}_\Theta{}^{\mathrm{T}} \rho c \frac{\Delta\Theta_i}{\Delta t} \,\mathrm{d}\Omega - \int_\Omega \boldsymbol{B}_\Theta{}^{\mathrm{T}} \boldsymbol{q}_i^{t+\Delta t} \,\mathrm{d}\Omega$$

and the left-hand side matrices are updated in each Newton-Raphson iteration.

It can be mathematically shown that finite element solution error for static analysis and non-stationary problem is bounded and tends to zero when finer spatial and time discretisations are applied. It is also mathematically proven that for backward Euler time integration the process is unconditionally stable (e.g. Quarteroni *et al*. (2000)).

4. DESCRIPTION OF COMPUTATIONAL TOOL

Building a new scientific simulation environment is a complex task. However, building own simulation tools gives the researchers an opportunity to shape them according to the new ideas that appear in computational science such as for instance meshless methods or XFEM.

In order to manage the complexity and the development costs of a simulation system a common approach is to use ready components, in particular Open Source Software. While code sharing is nothing new, we observe a steady shift towards component programming. This trend is fuelled by the appearance of many comprehensive, high quality software packages and improvement of standard interfaces between components.

The problem with selecting software components is such that when it turns out that a particular choice causes problems it is usually to late to modify it. The scope of the FEMDK project is solving multi-field problems that appear during the analysis of degradation phenomena of engineering materials with special attention paid to concrete. The main task is to build a problem-solving environment which would facilitate fast creation of tools for solving coupled problems. The environment should satisfy various requirements regarding data formats, geometric models, interpolation, solvers, etc.

The components of the constructed package FEMDK are presented in Putanowicz (2011), including FEM library `GetFEM++`, visualization libraries `VTK` and `HOOPS 3D`, mesh handling library `MOAB`, GUI library `Qt`, scripting extension language Python, configuration tool `CMake`, tools for handling scientific data and automation of multi language programming, solver libraries, tools for mesh generation and symbolic computing.

The present and future useful features of FEMDK are: arbitrary number of coupled fields, in other words arbitrary number of degrees of freedom per node (which also allows for XFEM extension); possibility of using different finite elements available in `GetFEM++` and different meshes for differently discretized fields; possibility of selecting particular algorithms, for instance for time or space integration, and for experimenting with new numerical algorithms; different nonlinear aspects of the model easily incorporated.

5. EXAMPLES

In this section examples are presented where selected thermo-elastic benchmark problems are analysed.

5.1. Strain and stress due to heat flow along a bar

In the first example a simple one-dimensional (1D) bar problem with stationary heat flow is analyzed in order to compare the results with an analytical solution. The 1D bar is 1 m long and supported at its both ends. The bar is subjected to imposed temperatures 250 °C and 0 °C at left and right ends, respectively. The material properties representative for aluminium alloy are selected and listed in table 1.

The Young modulus, thermal conductivity and coefficient of thermal expansion are either assumed to be constant as in table 1 or to depend on temperature in a piecewise linear manner as in table 2. In the latter case the analysis becomes nonlinear.

Figures 2–4 show the comparison of solutions obtained with constant material parameters, i.e. diagrams marked by "params=const" and temperature-dependent ones, i.e. diagrams marked by "params(T)". In figure 2 the temperature distributions are shown. In the nonlinear case the temperature is only slightly different from the standard one. Larger differences can be seen in the diagrams of the longitudinal displacement in figure 2, total and elastic strain in figure 3, and stress in figure 4 along the bar.

It can be seen in this simple example that the dependence of model parameters on temperature can play the important role in mechanical response. This is especially visible in figure 3 where for temperature-dependent Young modulus variable elastic strain distribution is predicted.

Table 1
Material properties

Name	Symbol	Value	Unit
Young modulus	E	$6.8948 \cdot 10^{10}$	Pa
Density	ρ	2720	kg/m^3
Poisson ratio	ν	0.35	
Linear expansion coefficient	α	$22.0 \cdot 10^{-6}$	m/(m·deg)
Thermal conductivity	k	205	W/(m·deg)

Table 2
Young modulus, thermal conductivity and linear expansion coefficient versus temperature

Temperature °C	0.0	93.0	149.0	250.0
Young modulus $\cdot 10^{10}$ Pa	6.8948	6.6190	6.3432	5.9985

Temperature °C	0.0	125.0	250.0
Thermal conductivity W/(m·deg)	205	215	250

Temperature °C	0.0	100.0	200.0	250.0
Linear expansion coefficient $\cdot 10^{-6}$ m/(m·deg)	22.0	25.4	26.5	27.15

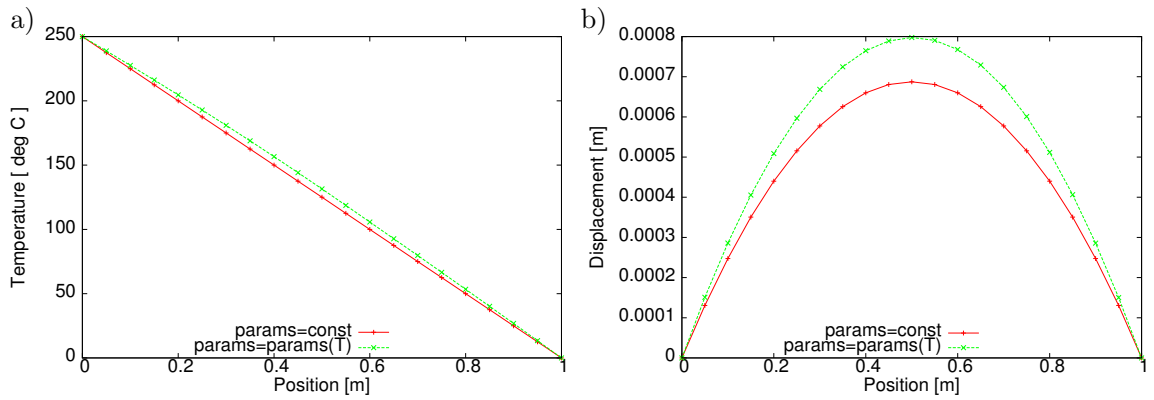

Fig. 2. Distribution of temperature a) and displacement b) along the bar

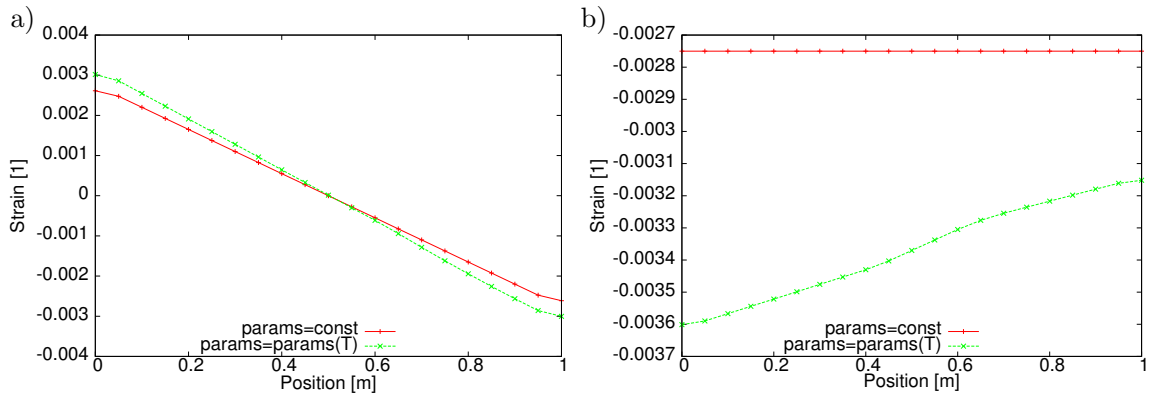

Fig. 3. Total strains a) and elastic strains b) along the bar

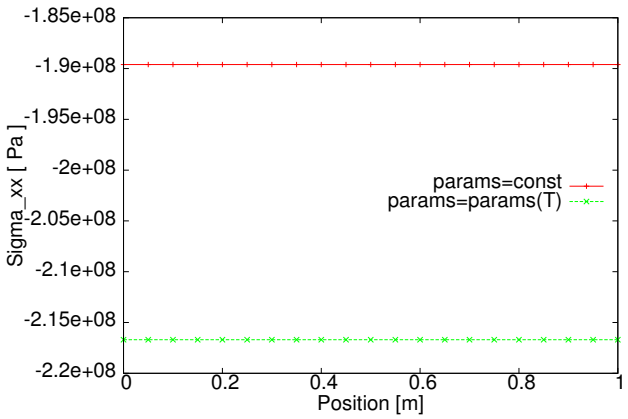

Fig. 4. Bar stresses

5.2. Thermal expansion of square configuration

In this example a two-dimensional specimen with arbitrary size 1 m $\times$ 1 m in plane strain conditions is considered. The configuration is mechanically supported and thermally loaded. The geometry and boundary conditions of mechanical and thermal kind are shown in figure 5. The material properties are assumed to be the same as in the previous example and are specified in tables 1–2. The thermal analysis is of stationary type.

Due to thermal expansion and mechanical constraints elastic strains and stresses occur in the panel. The temperature distribution along the horizontal axis is identical to the one shown in figure 2 for the 1D example in the previous subsection. There is indeed no change of temperature in vertical direction, see figure 6.

The displacement field for the nonlinear case is shown in figure 6. Similarly to the previous example the differences in results are significant for the strains, c.f. figure 7, although hardly visible in two-dimensional contour plots in figure 8.

5.3. Thick-walled pipe

In the example the nonstationary heat transfer in thick walled pipe in plain strain state is analized. The geometry and boundary conditions of the benchmark test are shown in figure 9. The natural boundary conditions for the mechanical subproblem are assumed to be homogeneous $p_{in} = p_{out} = 0$, so that the stresses in the cylinder are solely due to thermal expansion. The inner wall temperature grows in the transient analysis from $T(t_0) = 20$ deg. to $T = 200$ deg. at t_1=250 s and then it is constant until $t_2 = 500$ s. All material and load parameters are given in table 3. The results after final time step and after the first step at the beginning of the process are shown in figures 10 and 11.

Figure 10 shows several graphs illustrating temperature distribution in the cylinder. Due to the circular symmetry of the solution it is sufficient to illustrate temperature distribution along any radial line segment. Figure 10 shows the graphs for horizontal segment between $R = 5$ and $R = 6$ [m]. One can see high temperature gradient at the internal wall and relatively slow heat penetration with time. The final temperature distribution has the exponential character corresponding well to the analytical solution.

Closer scrutiny of numerical results reveals however occurrence of non-physical oscillations at the internal wall where high temperature gradients are present. The temperature drops below the initial temperature of 20° Celsius, which is physically not feasible since the pipe is heated. This effect can be traced back to the usage of finite elements with linear shape functions for temperature interpolation. With such functions one cannot properly resolve inside a single elements restrictions on temperature degrees of freedom resulting from high spatial gradient and coupling of degree-of-freedom (DOF) values in neighbouring nodes induced by the transient term. This situation is illustrated in figure 11 where the temperature graph in the vicinity of the internal boundary is shown.

Table 3
Material and load parameters for the thick-walled pipe example

Property	Symbol	Value	Unit
Density	ρ	2300	kg/m^3
Poisson ratio	ν	0.21	
Young modulus	E	32000	MPa
Coeff. of ther. expansion	α	10^{-5}	1/deg
Specific heat capacity	c	0.75	kJ/(kg K)
Thermal conductivity	k	1.7	W/(m K)
Reference temperature	T_0	0	°C
Inner wall pressure	p_{in}	0	Pa
Outer wall pressure	p_{ou}	0	Pa
Inner radius	R_{in}	5	m
Outer radius	R_{ou}	6	m

The application of a finer mesh does not solve the problem. With the finer mesh the spatial region with non-physical solution is smaller but the effect (that is the temperature drop below initial temperature) is more severe.

There are two possible remedies to regain the physical soundness of the solution. One is to use higher degree shape functions for the temperature field. The other solution is to keep linear shape functions for the temperature field but instead of using consistent thermal capacity matrix $\boldsymbol{C}$ (equivalent of the mass matrix in dynamics problem) one should use the lumped (i.e. diagonal) capacity matrix. The usage of the lumped matrix decouples the DOF values at neighbouring nodes for a single time step, which makes it possible to apply linear shape functions and obtain proper results. Figures 12, 13 and 14 show time variations of temperature, displacement and equivalent (Huber-Mises) stress at the central point of pipe wall ($R = 5.5$). The results obtained with linear and quadratic shape functions, both for consistent and lumped heat capacity matrices are compared. In figure 12 one can clearly see the inadmissible solution for linear elements and consistent capacity matrix. Figures 13 and 14 show the differences in displacement and stress fields induced by the differences in the temperature field for different shape functions or type of matrix $\boldsymbol{C}$. The results of this example show that even with such simple problem one should be careful about algorithmic details and should always do convergence study or by some other means assess the quality of numerical results. Depending on the particular problem at hand, non-physical or not fully convergent results can seriously undermine conclusions drawn from numerical simulations.

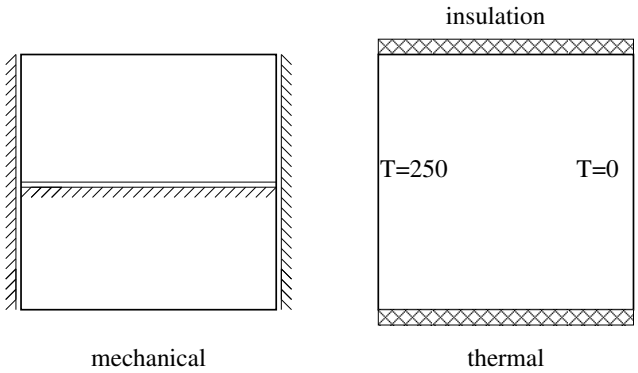

Fig. 5. Boundary conditions for square configuration

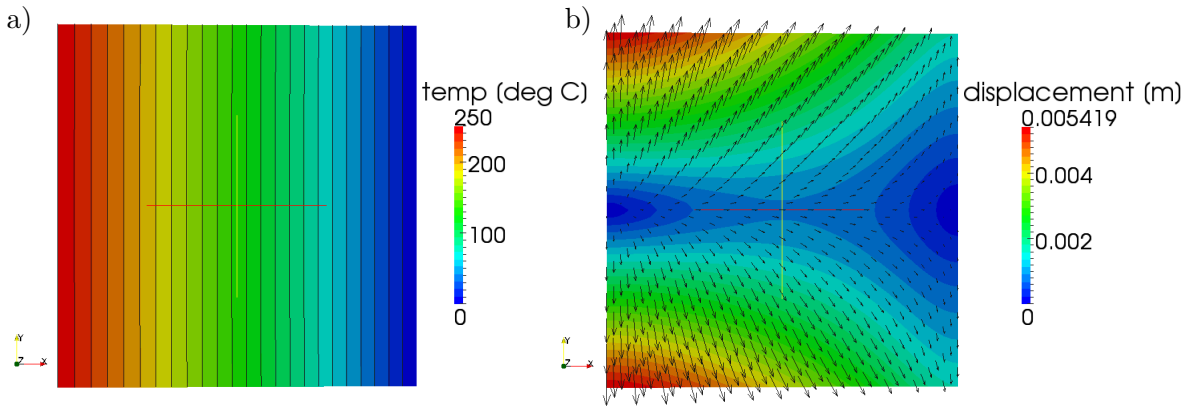

Fig. 6. Temperature distribution (a) and displacement field (b) in nonlinear analysis

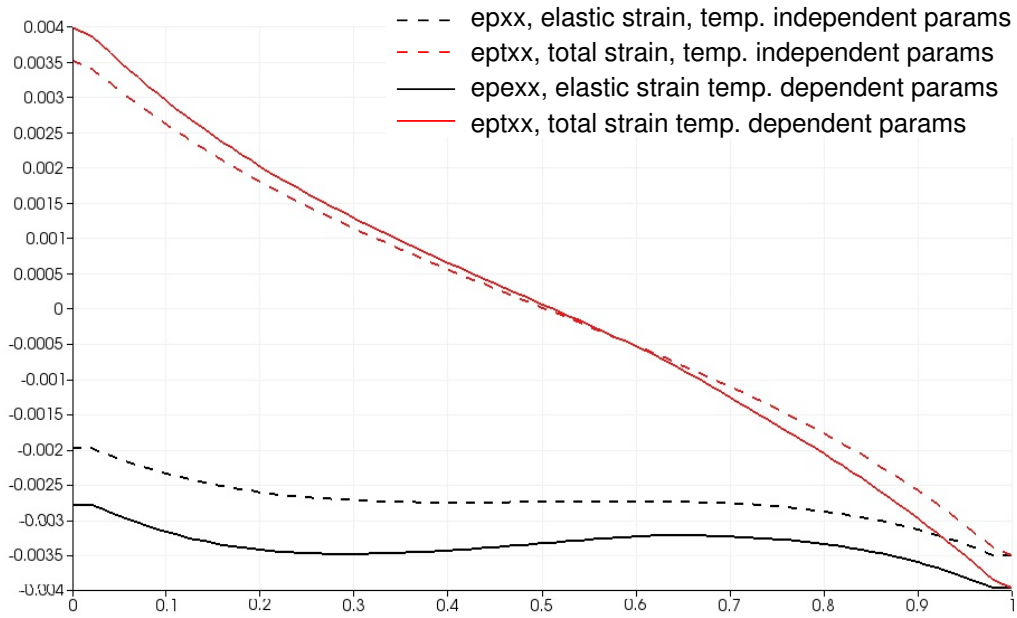

Fig. 7. Comparison of total strain distribution along horizontal symmetry axis

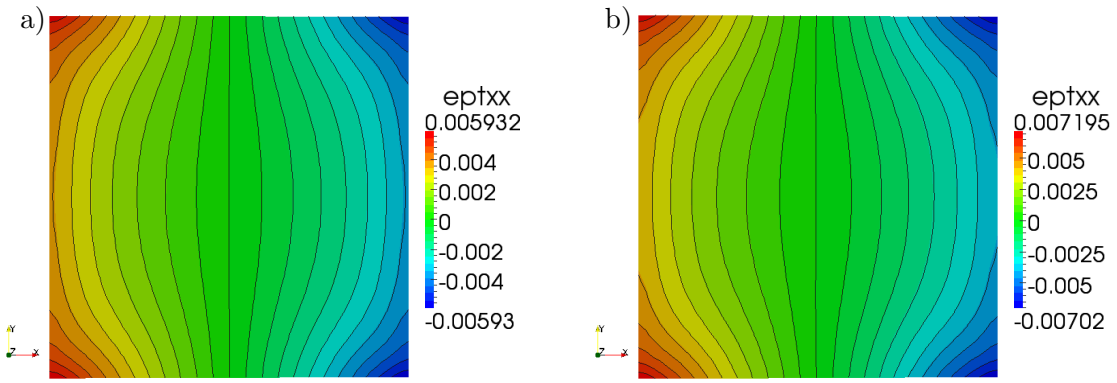

Fig. 8. Total strains ε_{xx} in linear (a) and nonlinear analysis (b)

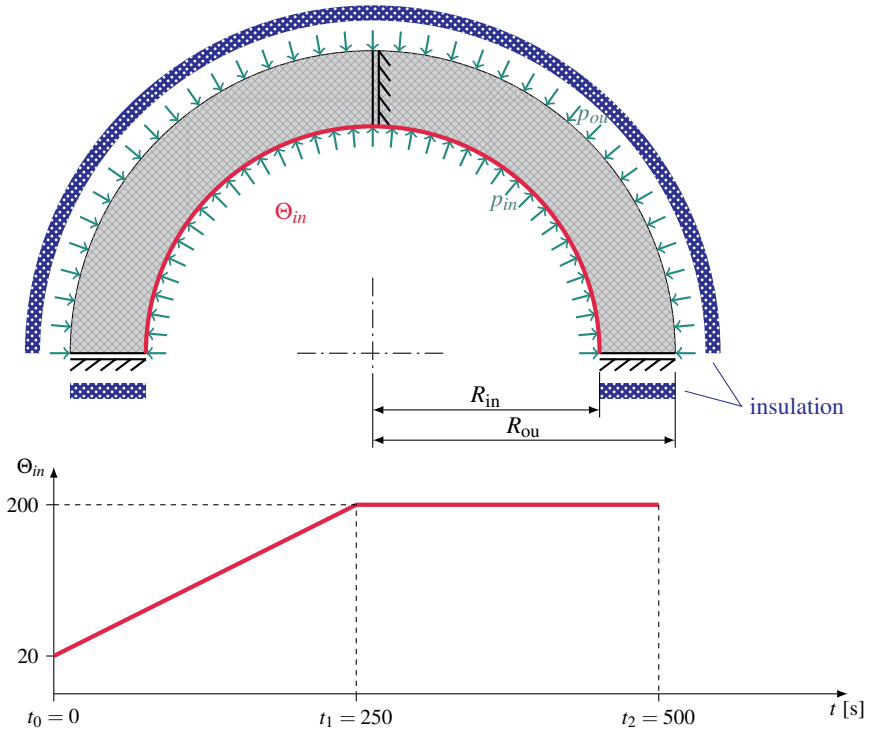

Fig. 9. Geometry and boundary conditions. Given temperature on inner boundary, insulation conditions on outer boundary

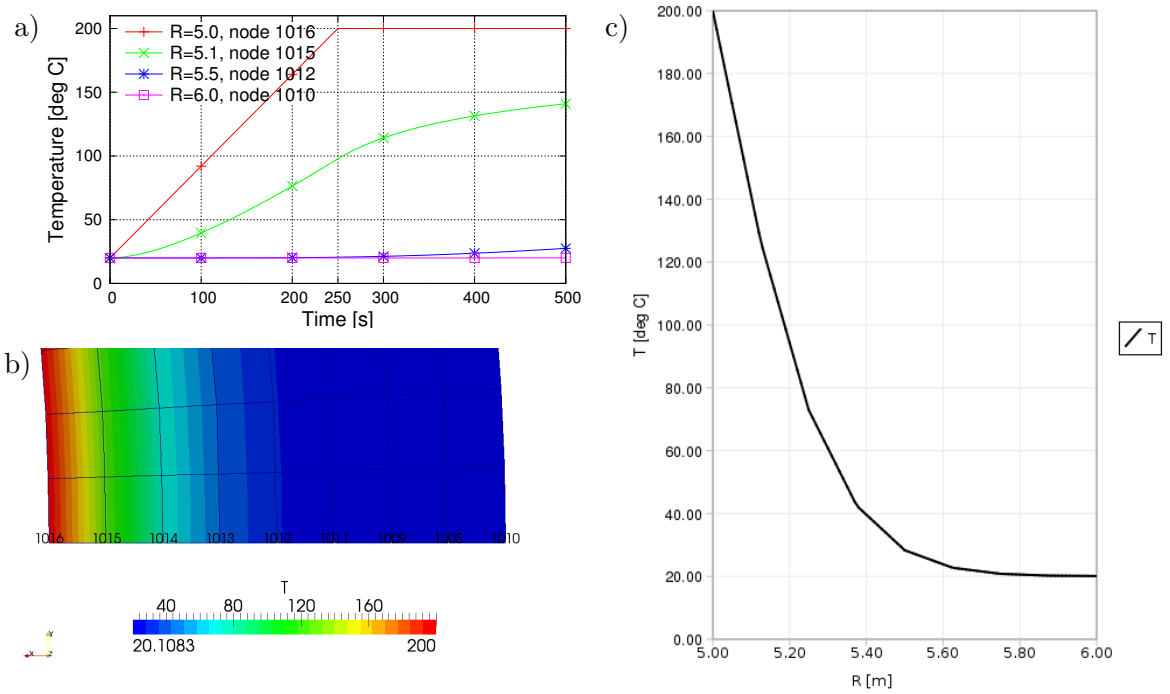

Fig. 10. Temperature evolution at nodes along the radius (a). Temperature distribution in the cylinder with marked nodes (b). Solution for the last time step, $t = 500\,\mathrm{s}$ (c)

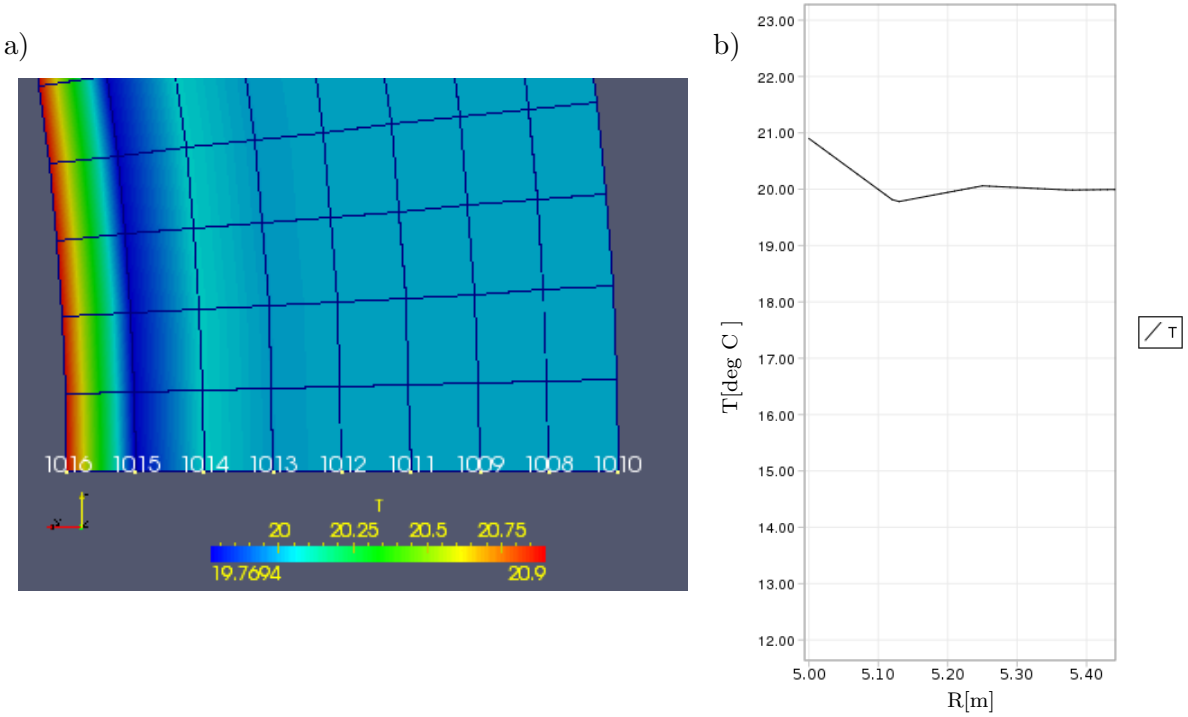

Fig. 11. Solution for the first time step: temperature distribution in the cylinder

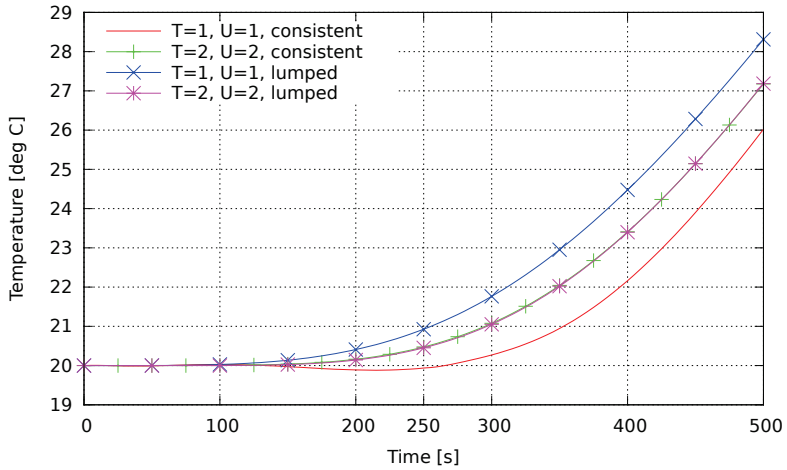

Fig. 12. Temperature history at pipe middle-surface

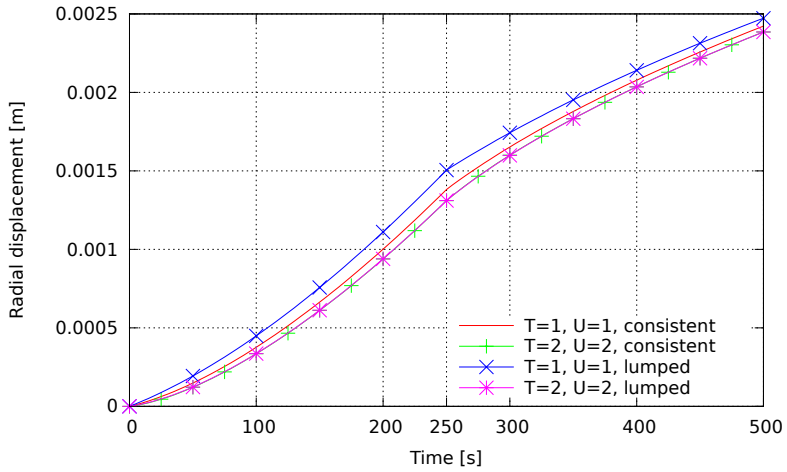

Fig. 13. Displacement history at pipe middle-surface

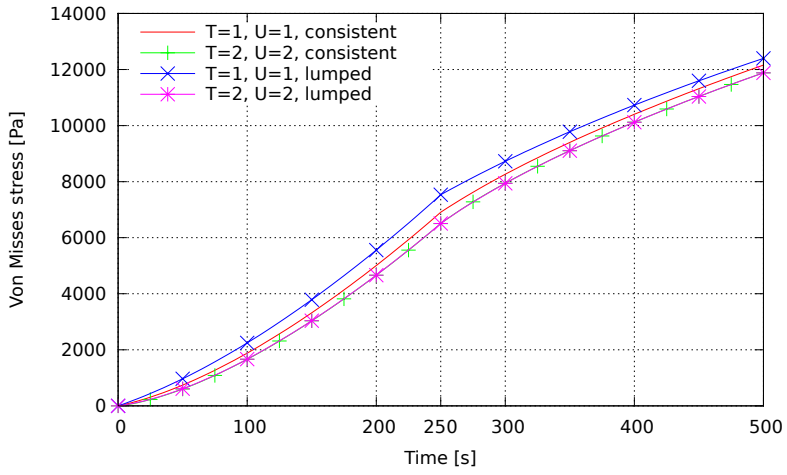

Fig. 14. Huber-Mises stress history at pipe middle-surface

6. CONCLUSIONS AND FUTURE WORK

In the paper the research on thermo-elasticity as typical coupling of diffusion and momentum balance has been described. The approach has a theoretical-numerical character, focused on finite element approximation. The theory and algorithm including nonlinear elasticity, linearization and time integration has been derived. Some benchmark tests which can be used for the verification of existing or developed software have been described.

For the problems analysed in this paper model parameters depend on current temperature distribution. This complicates the analysis of the errors a priori. It is not the main aim of the paper to perform complete error analysis of such kind of problems.

On the other hand the influence of truncation errors on obtained results needs to be taken into account during analysis.

In the examples presented in this paper various densities of spatial and time discretisations have been applied. It has been noticed that the discretisation levels have a mere influence on the obtained results. On the basis of that it can be concluded that in the examples presented in this paper the proposed approximation procedures do not generate errors of the order that would have a great impact on the results.

Solving coupled problems is nowadays a common theme in numerical simulations. Thermo-mechanical coupling is one of the simplest problems, as the physics behind it is well understood. From numerical simulations point of view this case is important as its implementation can be used as a model and reference point for more complex cases. The paper shows how the base case can be extended by taking into account spatial and temporal variation of problem parameters, as well as the nonlinear character of the thermal problem when the material properties depend on temperature.

With an appropriate FEM application the introduction of parameters variability or nonlinear mode is just a matter of couple of mouse clicks or a switch in data file. However, when writing an implementation one has to plan ahead in order not to patch the program code in an ad-hoc manner, which can lead to unmanageable program code. The provisions for possible extensions turn out to be the crucial point. In the similar spirit, the full control of algorithm parameters such as finite element interpolation, integration type and quadrature order, separate meshes for different fields, is crucial for making complete investigation of problem at hand. The tools that were used for building the applications for the presented examples have shown the required level of flexibility. The choice of `GetFEM++` library as FEM engine, despite the high overhead due to complexity of object and generic programming in C++, looks like a good decision. The theory and examples presented in this paper can serve as the base for mastering `GetFEM++` library, providing a reference point.

The theory can be extended to thermo-plasticity, see e.g. Jaśkowiec *et al*. (2012); Ottosen and Ristinmaa (2005), where full coupling between mechanics and heat transfer is described due to plastic dissipation and a monolithic solution scheme similar to the one presented in eq. (50) is mandatory. This research can also be continued in many other directions. For instance, one can derive the formulation of plane stress and axisymmetric models (in the former case the constraint $\sigma_{zz} = 0$ must be imposed which is not always trivial for coupled theories). Concerning FEM, the analysis of proper balance of interpolations for the coupled fields seems important, cf. Zienkiewicz *et al*. (2005). Finally, the incorporation of additional coupled fields (the first candidate is fluid diffusion) seems necessary in order to be able to simulate important real-life problems, e.g. material behaviour in fire conditions or corrosion processes.

Acknowledgement

The scientific research presented in this paper has been partly carried out within the project "Innovative recourses and effective methods of safety improvement and durability of buildings and transport infrastructure in the sustainable development" financed by the European Union from the European Fund of Regional Development based on the Operational Program of the Innovative Economy. Moreover, the financial support of the Polish Ministry of Science and Higher Education within contract L5/104/2013/DS is gratefully acknowledged.

References

Buckley D. 2010, *Solution of Nonlinear Transient Heat Transfer Problems*. M.Sc. thesis, Florida International University, Miami, Florida, FIU Electronic Theses and Dissertation. Paper 302.

Gawin D. 2010, *Degradation processes in microstructure of cement composites at high temperature* (in Polish). Engineering studies no 69, Polish Academy of Sciences, Warsaw.

Jaśkowiec J., Plucński P., Putanowicz R., Stankiewicz A., Wosatko A., Pamin J. 2012, *Formulation and FEM implementation of nonlinear thermo-mechanical coupling*. In Pęcherski R. *et al.*, editors, Proc. 38th Solid Mechanics Conference SolMech 2012, pages 36–37, Warszawa. IFTR Reports.

Jirasek M., Bažant Z.P. 2002, *Inelastic Analysis of Structures*. J. Wiley & Sons, Chichester.

Kubik J. 2004, *Elements of thermomechanics* (in Polish). Technical report, Opole University of Technology, Opole.

Kuhl D. 2005, *Modellierung und Simulation von Mehrfeldproblemen der Strukturmechanik*. Dissertation, Ruhr University of Bochum.

Lemaitre J., Chaboche J.L. 1990, *Mechanics of Solid Materials*. Cambridge University Press, Cambridge.

Lubliner J. 1990, *Plasticity Theory*. Macmillan Publishing Company, New York.

Maugin G.A. 1992, *The Thermomechanics of Plasticity and Fracture*. Cambridge University Press, Cambridge.

Nicholson D. 2008, *Finite element analysis. Theromechanics of solids*. CRC Press, Boca Raton.

Ottosen N.S., Ristinmaa M. 2005, *The Mechanics of Constitutive Modeling*. Elsevier.

Putanowicz R. 2011, *Grounds for the selection of software components for building FEM simulation systems for coupled problems.* Mechanics and Control, 30(4):234–244.

Quarteroni A., Sacco R., Saleri F. 2000, *Numerical Mathematics*. Texts in Applied Mathematics Series. Springer-Verlag GmbH.

Zienkiewicz O.C., Taylor R.L., Zhu J.Z. 2005, *The Finite Element Method: Its Basis and Fundamentals*. Elsevier Butterworth-Heinemann, sixth edition.